

M2I2: Learning Efficient Multi-Agent Communication via Masked State Modeling and Intention Inference

Chuxiong Sun^{1 2 *}, Peng He^{4 1 *}, Qirui Ji^{1 3 *}, Zehua Zang^{1 3},
Jiangmeng Li^{1 2 †}, Rui Wang^{1 2}, Wei Wang⁴

¹National Key Laboratory of Space Integrated Information System, Institute of Software Chinese Academy of Sciences

²State Key Laboratory of Intelligent Game

³University of Chinese Academy of Sciences

⁴Beijing University of Posts and Telecommunications

{chuxiong2016, jqirui2022, zehua2020, wangrui, jiangmeng2019}@iscas.ac.cn, {hepeng123, weiwang}@bupt.edu.cn

Abstract

Communication is essential in coordinating the behaviors of multiple agents. However, existing methods primarily emphasize content, timing, and partners for information sharing, often neglecting the critical aspect of integrating shared information. This gap can significantly impact agents' ability to understand and respond to complex, uncertain interactions, thus affecting overall communication efficiency. To address this issue, we introduce M2I2, a novel framework designed to enhance the agents' capabilities to assimilate and utilize received information effectively. M2I2 equips agents with advanced capabilities for masked state modeling and joint-action prediction, enriching their perception of environmental uncertainties and facilitating the anticipation of teammates' intentions. This approach ensures that agents are furnished with both comprehensive and relevant information, bolstering more informed and synergistic behaviors. Moreover, we propose a Dimensional Rational Network, innovatively trained via a meta-learning paradigm, to identify the importance of dimensional pieces of information, evaluating their contributions to decision-making and auxiliary tasks. Then, we implement an importance-based heuristic for selective information masking and sharing. This strategy optimizes the efficiency of masked state modeling and the rationale behind information sharing. We evaluate M2I2 across diverse multi-agent tasks, and the results demonstrate its superior performance, efficiency, and generalization capabilities, over existing state-of-the-art methods in various complex scenarios.

1 Introduction

Reinforcement Learning (RL) has achieved significant milestones in various complex real-world applications, from Game AI (Osband et al. 2016; Silver et al. 2017, 2018; Vinyals et al. 2019) and Robotics (Andrychowicz et al. 2020) to Autonomous Driving (Leurent 2018). However, the landscape shifts markedly when applied to Multi-Agent Reinforcement Learning (MAREL) (Lowe et al. 2017; Rashid et al. 2018; Yu et al. 2022), where unique challenges emerge. A principal challenge is the issue of partial observability, where agents must make decisions based on limited local ob-

servations, lacking a comprehensive view of the entire environment. In addressing this challenge, multi-agent communication emerges as a potent solution. By enabling agents to *share* and *integrate* information, this strategy facilitates a deeper collective understanding of their environment, stabilizing the learning process and promoting synchronized actions among agents.

Despite advancements, existing methods in multi-agent communication primarily focus on sending policies, such as creating meaningful messages (Zhang, Zhang, and Lin 2019, 2020; Yuan et al. 2022), optimizing the timing (Singh, Jain, and Sukhbaatar 2018; Kim et al. 2019) and selecting appropriate partners (Ding, Huang, and Lu 2020; Niu, Paleja, and Gombolay 2021; Xue et al. 2022) for information exchange. However, these methods exhibit a significant gap in effectively integrating received information to enhance decision-making at receiving end. Typically, a large volume of received messages, processed by basic mechanisms like concatenation (Sukhbaatar, Szlam, and Fergus 2016) is fed directly into policy networks. This approach treats the information integration task as a black box, presupposing that neural networks can autonomously discern the most decision-important information, overlooking the intricacies of cognition and collaborative decision-making. In contrast, human cognitive processes (Etel and Slaughter 2019) demonstrate a superior ability for utilizing received information to perceive the environment and reduce the uncertainty of decision-making. This level of decision-making complexity, inherent in human cognition, is something that current multi-agent communication methods fail to capture.

Inspired by human cognitive processes and recent advancements in representation learning, as illustrated by models like BERT (Devlin et al. 2019) and MAE (He et al. 2022), we redefine the challenge of information integration in multi-agent communication as one of representation learning task. In this context, agents are tasked with developing representations for cooperative decision-making from a limited set of messages. These messages, constrained by partial observability and limited communication resources, only reflect a subset of the environmental states, often proving inadequate for a comprehensive understanding of environmental dynamics. Furthermore, not all received mes-

*These authors contributed equally.

†Corresponding author.

sages are beneficial for decision-making; some may introduce noise that disrupts the process. Consequently, we argue that an ideal representation in this context must be both **sufficient**—offering a comprehensive breadth of information for a deep understanding of the environment, and **informative**—sharply focused on data crucial for facilitating cooperative decision-making.

Following this principle, we introduce M2I2, a novel approach incorporating two self-supervised auxiliary tasks to enhance efficiency of information integration. To meet the standard of “sufficient”, M2I2 utilizes masked modeling techniques to reconstruct global states from received messages, furnishing agents with comprehensive information for informed decision-making. Essentially, M2I2 introduces a state-level Masked Auto-Encoder (MAE) designed for multi-agent communication. A distinctive aspect of this model is its unique masking mechanism, where the masks are dynamically determined by the communication strategies of the sending agents. Our empirical studies highlight that traditional random mask generating techniques (Devlin et al. 2019; He et al. 2022; Liu et al. 2022) fall short in addressing the complexities encountered in MARL. To this end, we develop the Dimensional Rational Network (DRN) to dynamically adjust the importance of each dimension of observed information. DRN is trained via a meta-learning paradigm, which takes into account the impacts on both decision-making and auxiliary tasks. After exploring the rationale of dimensional observations, we further propose an importance-based heuristic to discern which dimensions of observations should be masked at both training and execution stages, thereby enhancing the efficiency of masked state modeling and communication rationality.

Regarding the “informative” aspect, M2I2 integrates an inverse model to predict joint actions from sequential state representations, enabling agents to focus on information pivotal to their decisions. Furthermore, the inverse model enables agents to infer their teammates’ intentions during decentralized decision-making processes. This capability is essential for facilitating team communication that goes beyond mere information exchange, enabling a deeper understanding of teammates’ intentions and insights that can impact collective strategies. By introducing the self-supervised objective, M2I2 facilitates a deeper integration of received information, allowing agents to align closely with each other’s intentions and leading to more efficient and informed decision-making across various scenarios.

To validate the effectiveness of M2I2, we conduct comprehensive evaluations across a range of multi-agent tasks with differing complexities, from Hallway and MPE to SMAC. Compared to state-of-the-art communication methods (Das et al. 2019; Yuan et al. 2022; Xue et al. 2022; Guan et al. 2022), M2I2 demonstrates superior performance, enhanced efficiency, and remarkable generalization capabilities. Our main **contributions** are summarized in three-fold:

- To the best of our knowledge, M2I2 represents the first instance of incorporating self-supervised objectives, i.e., reconstructing global states and predicting joint actions, into the process of information integration under the condition of partial observability and restricted communica-

tion resources.

- We integrate a meta-learning paradigm to model the contribution of each dimensional piece of information towards both decision-making and self-supervised objectives, therefore directing agents to transmit and focus on only the most relevant and important information.
- Empirically, our proposed method not only facilitates efficient message integration, but also significantly improves communication efficiency, effectively bridging a vital research gap in MARL.

2 Related Works

Multi-agent communication has emerged as an indispensable component in MARL. Research in this domain has primarily concentrated on three fundamental questions:

Determining the optimal content of communication (what to communicate). CommNet (Sukhbaatar, Szlam, and Fergus 2016), as a pioneering work in this area, facilitated agents in learning continuous messages. Following CommNet, several methods have been developed to further refine the message learning process. VBC (Zhang, Zhang, and Lin 2019) aims to filter out noisy parts while retaining valuable content by limiting the variance of messages. TMC (Zhang, Zhang, and Lin 2020) introduces regularizers to reduce temporally redundant messages. NDQ (Wang et al. 2020) employs information-theoretic regularizers to develop expressive and succinct messages. MAIC (Yuan et al. 2022) enabled agents to customize communications for specific recipients, advancing tailored message learning.

Deciding appropriate timing and partners for information exchange (when and whom to communicate). To enhance communication efficiency, approaches such as IC3Net (Singh, Jain, and Sukhbaatar 2018) and ATOC (Kim et al. 2019) have introduced gating networks to eliminate superfluous communication links. Similarly, SchedNet (Kim et al. 2019) and IMMAC (Sun et al. 2021) have modeled the significance of observations, using heuristic mechanisms to gate non-essential communication. Further, methods such as MAGIC (Niu, Paleja, and Gombolay 2021), I2C (Ding, Huang, and Lu 2020) and SMS (Xue et al. 2022) have been developed to identify the most suitable recipients. These approaches focus on modeling the contribution of shared information to the decision-making processes of the recipients, aiming to direct communication where it most influences decision-making.

Integrating incoming messages and making decisions (how to utilize received information). TarMAC (Das et al. 2019) has explored how agents can effectively assimilate crucial information from an abundance of raw messages. MASIA (Guan et al. 2022) take a different approach, employing an Auto-Encoder and a forward model for information integration and becoming the first to introduce self-supervised learning into multi-agent communication. However, MASIA is under the strong assumption that agents have access to all observations from their peers. In this work, we challenge and relax this assumption by introducing the masked state modeling technique, extending the approach

to more realistic environments where communication resources are constrained.

Furthermore, our work is also related to the mask modeling techniques (He et al. 2022; Devlin et al. 2019; Liu et al. 2022). However, M2I2 is the first to apply this approach within the multi-agent communication domain, utilizing this technique to effectively tackle the challenge of imperfect information that arises from constrained communication resources. A key distinction of M2I2 lies in its innovative masking mechanism, which differs significantly from those used in prior methods. This unique approach will be elaborated upon in **Section 4.4**.

3 Preliminary

In this work, we focus on fully cooperative multi-agent tasks, characterized by partial observability and necessity for inter-agent communication. These tasks are modeled as Decentralized Partially Observable Markov Decision Processes (Dec-POMDPs) (Oliehoek, Amato et al. 2016), represented by the tuple $G = (N, S, O, A, \odot, P, R, \gamma, M)$. In this formulation, $N \equiv \{1, \dots, n\}$ denotes the set of agents, S represents the global states, O describes the observations available to each agent, A signifies the set of available actions, \odot is the observation function mapping states to observations, P is the transition function illustrating the dynamics of the environment, R is the reward function dependent on the global states and joint actions of the agents, γ is the discount factor, and M specifies the set of messages that can be communicated among the agents. At each time-step t , each agent $i \in N$ has access to its own observation $o_i^t \in O$ determined by the observation function $\odot(o_i^t|s_t)$. Additionally, each agent can receive messages $c_i^t = \sum_{j \neq i} m_j^t$ from teammates $j \in N$. Utilizing both the observed and received information, agents then make local decisions. As each agent selects an action, the joint action a_t results in a shared reward $r_t = R(s_t, a_t)$ and transitions the system to the next state s_{t+1} according to the transition function $P(s_{t+1}|s_t, a_t)$. The objective for all agents is to collaboratively develop a joint policy π to maximize the discounted cumulative return $\sum_{t=0}^{\infty} \gamma^t r_t$.

Centralized Training with Decentralized Execution (CTDE) (Lowe et al. 2017) stands as a promising paradigm in cooperative multi-agent tasks. Within this paradigm, individual agents make decisions based on local information, while their policies are trained through a centralized manager with access to global information. This work aligns with the prevailing value-based approaches within the CTDE framework. During the training phase, the joint action-value function $Q_{tot}(s_t, a_t; \theta)$ will be trained to minimize the expected Temporal Difference (TD) error:

$$\mathcal{L}_{RL}(\theta) = \mathbb{E}_{s_t, a_t, r_t, s_{t+1} \in D} [y_t - Q_{tot}(s_t, a_t; \theta)]^2, \quad (1)$$

where D is the replay buffer, $y_t = r_t + \gamma \max_{a_{t+1}} Q_{tot}(s_{t+1}, a_{t+1}; \theta^-)$ is the TD target. θ^- denotes the parameters of the target network, which is periodically updated by θ .

4 Methodology

4.1 Overall Framework

The framework of M2I2 are shown in Figure 1, with its core components highlighted for effective multi-agent communication. A key component of M2I2 includes a message encoder and a state decoder, functioning collectively as an extendable module to reconstruct the environmental states in an auto-encoding manner. This design allows for the reconstruction of global states from received messages (i.e. limited observations), thereby providing agents with sufficient information to make well-informed cooperative decisions. Furthermore, M2I2 integrates an inverse model capable of predicting joint actions based on consecutive state representations. This model is pivotal in equipping agents with the ability to infer the intentions of their teammates while making decisions. Another standout feature of M2I2 is DRN, which is adept at evaluating the importance of various observed information based on their gradient contributions to both auxiliary and RL tasks. The DRN is continually refined through a meta-learning paradigm, which effectively avoid the trivial solution and local optimum issues during training. By identifying and emphasizing important information, DRN enables agents to share and focus on important data, thereby optimizing the communication process for efficiency and effectiveness.

4.2 Communication Process of M2I2

The communication process of M2I2 can be summarized as the following four steps.

Selectively masking unnecessary observations for information sharing: At each time-step, agents utilize the DRN to evaluate the importance of observed information in supporting decision-making and auxiliary tasks. This importance is quantified as $\omega_i = \omega_{id} | d \in [1, D]$, where i represents the ID of the agent and D is the dimensionality of observed information. To optimize communication efficiency while ensuring effective decision-making, a topK mechanism is applied for generating observation masks, which is formulated as:

$$\text{topK}(\omega_i) = \begin{cases} \omega_{id}, & \text{if } d \text{ in top-k largest dimensions} \\ 0, & \text{others.} \end{cases} \quad (2)$$

This process allows each agent to selectively share the most important dimensions of the observations while non-essential dimensions are masked to zero. The resulting shared information is represented as:

$$m_i^t = o_i^t \otimes \text{topK}(\omega_i), \quad (3)$$

where m_i^t denotes the messages, i.e. masked and weighted observations, and \otimes is an element-wise Hadamard product function. The DRN, central to this selectively observation mask process, is trained using a meta-learning paradigm (detailed in **Section 4.4**), which enables it to dynamically adjust its assessments based on both decision-making and auxiliary task performances.

Integrating received information: Upon receiving messages, M2I2 integrates a scaled dot-product self-attention

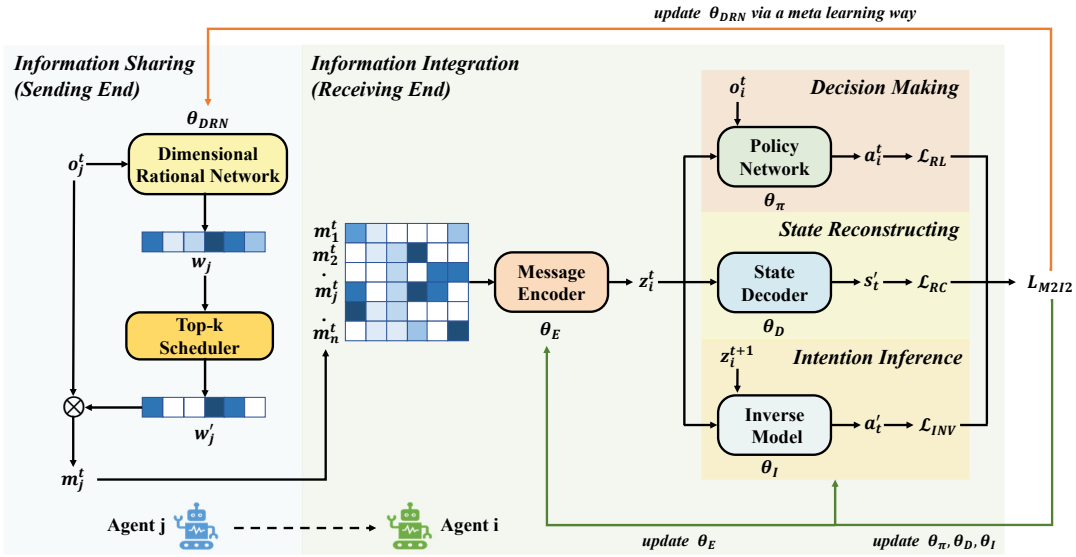


Figure 1: Framework of M2I2. Similar to other CTDE approaches in MARL, M2I2 only leverages global states and joint actions during centralized training phase. However, M2I2 distinguishes itself through its self-supervised auxiliary tasks. These tasks enable agents to develop representations from received messages, enhancing their ability to comprehend global states and infer teammates’ joint actions. This capability becomes particularly valuable during the decentralized execution phase, where agents must operate based on limited observations.

module (Vaswani et al. 2017) to adeptly process incoming messages. Specifically, the received messages are transformed into corresponding queries Q , keys K , and values V . The process of integrating this information is mathematically represented as follows:

$$z_i^t = f_{\theta_E}(\text{softmax}(\frac{QK^T}{\sqrt{D_k}})V) \quad (4)$$

where θ_E represents the parameters of Message Encoder and D_k represents the dimension of a single key. This message encoder exhibits two notable benefits. Firstly, the encoder’s design makes it adaptable to diverse communication contexts, accommodating varying numbers and arrangements of agents. Secondly, by utilizing a weighted sum mechanism, the self-attention module integrates information without excessively expanding the agents’ local policy spaces.

Implicitly Inferring the global states and teammates’ intention: Following this, M2I2 encode the received messages into a compact representation. Unlike traditional methods that rely solely on RL objectives, which often struggle to learn effective representation from the limited and noisy messages, M2I2 incorporates two self-supervised objectives. These objectives are specifically designed to develop a representation that is both “sufficient” for a thorough understanding of the environment and “promising” for aiding cooperative decision-making. *Although the involved self-supervised auxiliary tasks are conducted only during training, they can implicitly enhance the message encoder’s ability to interpret the environment and predict teammates’ intentions during decentralized decision-making process.*

Making cooperative decisions: The culmination of the M2I2 process is reflected in the agents’ ability to make co-

operative decisions. Here, the enriched integrated information, blended with each agent’s personal observations, is channeled into the policy network. The process of decision-making is mathematically represented as follows:

$$a_i^t = \pi_i(o_i^t, z_i^t; \theta_\pi) \quad (5)$$

where θ_π represents the parameters of policy network. This convergence of individual perception and collective insights is crucial, as it empowers agents to make decisions that are not only informed, but also aligned with the overarching goals and strategies of the team.

4.3 Self-Supervised Auxiliary Tasks for Efficient Multi-Agent Communication

Given the inherent constraints in agents’ perceptual capabilities and the limitations of communication bandwidth, the information encoded by the message encoder often captures only a fraction of the environment’s state. To ensure that agents have access to sufficient information for effective decision-making, we employ a state decoder. This decoder is tasked with reconstructing the global state of the environment, represented by $s_i^t = g_{\theta_D}(z_i^t)$. The associated loss function is computed using the mean squared error between the reconstructed and global states:

$$\mathcal{L}_{RC}(\theta_E, \theta_D) = \mathbb{E}_{z_i^t, s_i^t} \|s_i^t - s_i^t\|_2^2. \quad (6)$$

By combining the message encoder with the state decoder, we effectively create an extendable masked state modeling. This masked modeling is characterized by a unique masking process, generated both by the environment and the agents themselves. This approach enables the integrated representation z_i^t to effectively represent the global states of the en-

vironment, thus overcoming the challenges posed by their limited observational scope and communication capacity.

To augment the capability of agents in focusing on information promising to their decisions and aligning with the intentions of their counterparts, we introduce an inverse model, denoted as $I_{\theta_I} : \mathcal{Z} \times \mathcal{Z} \rightarrow A^n$, where \mathcal{Z} is the space of state representations. This model is crafted to predict the joint actions that agents take to transition from one state representation to the next. Formally, given a triplet (z_t, a_t, z_{t+1}) composed of two consecutive state representations and joint actions taken by agents, we parameterise the conditional likelihood as $p(a'_t) = I_{\theta_I}(z_t, z_{t+1})$, where I_{θ_I} embodies a two hidden layers MLP followed by a softmax operation. The parameters of both inverse model θ_I and message encoder θ_E are optimized via a maximum likelihood approach. The corresponding loss function is formulated as:

$$\mathcal{L}_{INV}(\theta_E, \theta_I) = \mathbb{E}_{z'_t, a_t} \|a'_t - a_t\|_2^2, \quad (7)$$

where this loss function measures the discrepancy between the predicted joint actions and the actual joint actions. At first, the objective encourages agents to focus on information that are controllable and expressive pertinent to cooperative decision-making. This focus is crucial for agents to effectively handle elements that they can influence, enhancing their relevance in a coordinated environment. Moreover, the deeper integration of received information facilitated by the model allows agents to implicitly infer the intentions of others during execution. This capability significantly bolsters agents' potential to align their actions with the intentions of their teammates. Such alignment is not only technically beneficial, but also aligns with cognitive research findings (Etel and Slaughter 2019), which underscore the importance of intention understanding in effective social interactions.

4.4 DRN for Importance Modeling

DRN is designed to discern the importance of different dimensions of observed information, specifically tailoring to the needs of decision-making and auxiliary tasks. The primary challenge here lies in the dynamic nature of the MARL and the variability in communication needs across different stages of a mission. Unlike static scenarios, the importance of information can change dramatically, requiring the DRN to adapt continuously and efficiently. This challenge transcends the realm of simple optimization problems, typically addressed with first-order gradients. To effectively navigate this complexity, we employ a meta-learning approach (Liu, Davison, and Johns 2019), as it is well-suited to circumvent trivial solutions and local optima that often hinder training efficiency. It allows the DRN to dynamically adjust its understanding of information importance in a sophisticated manner, aligning closely with the overarching goals of decision-making and auxiliary tasks.

It is important to note that within our training framework, only the parameters of θ_{DRN} are refined using this meta-learning approach. The other parameters of the system are updated using conventional first-order gradient methods. Specifically, in the first regular training step, we focus on training the combined set of parameters $\theta = (\theta_E, \theta_D, \theta_I, \theta_\pi)$

by jointly minimizing the auxiliary tasks and RL losses, which is formalized by

$$\arg \min_{\theta} \mathcal{L}_{M2I2}(\theta, \theta_{DRN}), \quad (8)$$

where $\mathcal{L}_{M2I2}(\theta, \theta_{DRN}) = \mathcal{L}_{RL} + \beta(\mathcal{L}_{RC} + \mathcal{L}_{INV})$ and β is a coefficient that controls the balance between RL objective and auxiliary objectives.

In the second meta-learning-based step, θ_{DRN} is updated by using the second-derivative technique (Liu, Davison, and Johns 2019; Li et al. 2022). This technique is crucial for adjusting θ_{DRN} to better discern the importance of various information dimensions that significantly impact both RL and auxiliary tasks. The update process involves calculating the gradients of θ_{DRN} in relation to the combined performance metrics from these tasks, encapsulated by \mathcal{L}_{M2I2} . Formally, we update θ_{DRN} by

$$\arg \min_{\theta_{DRN}} \mathcal{L}_{M2I2}(\theta_{trial}, \theta_{DRN}), \quad (9)$$

where $\theta_{trial} = (\theta_E^{trial}, \theta_D^{trial}, \theta_I^{trial}, \theta_\pi^{trial})$ is the trial weights of the θ after one gradient update using the M2I2 loss defined in Equation 8. We formulate the updating of such trial weights as follows:

$$\theta_{trial} = \theta - \ell_\theta \nabla_{\theta} \mathcal{L}_{M2I2}, \quad (10)$$

where ℓ_θ is the learning rate. Note that the calculation of trial weights excludes the step of gradient back-propagation. Thus, θ_{DRN} is updated through the second-derivative gradient of θ . By doing so, we ensure that θ_{DRN} is continuously fine-tuned by the gradient contributions of \mathcal{L}_{M2I2} , allowing DRN to dynamically evaluate the importance of each observed dimension. Our visualization study in **Appendix D** further validates this approach: it reveals that the DRN not only distinguishes varying levels of importance across different agent types and observation categories but also dynamically adjusts these importance weights over time, adapting to the evolving demands of the task.

5 Experiment

In this section, our experimental design is meticulously structured to address three fundamental questions:

- **RQ1.** How does M2I2's performance and efficiency compare to leading communication methods?
- **RQ2.** What specific components within M2I2 are instrumental to its performance?
- **RQ3.** Is M2I2 versatile enough to be applied across a range of tasks, and can it be seamlessly integrated with multiple existing baselines?

5.1 Setup

Benchmarks. In order to demonstrate the effectiveness and generality of M2I2, we conducted extensive experiments across four popular multi-agent communication benchmarks: Hallway (Wang et al. 2020), Predator-Prey (PP) (Lowe et al. 2017), SMAC (Samvelyan et al. 2019) and SMAC-Communication (Wang et al. 2020). Each of these benchmarks provides a substantial testbed for evaluating

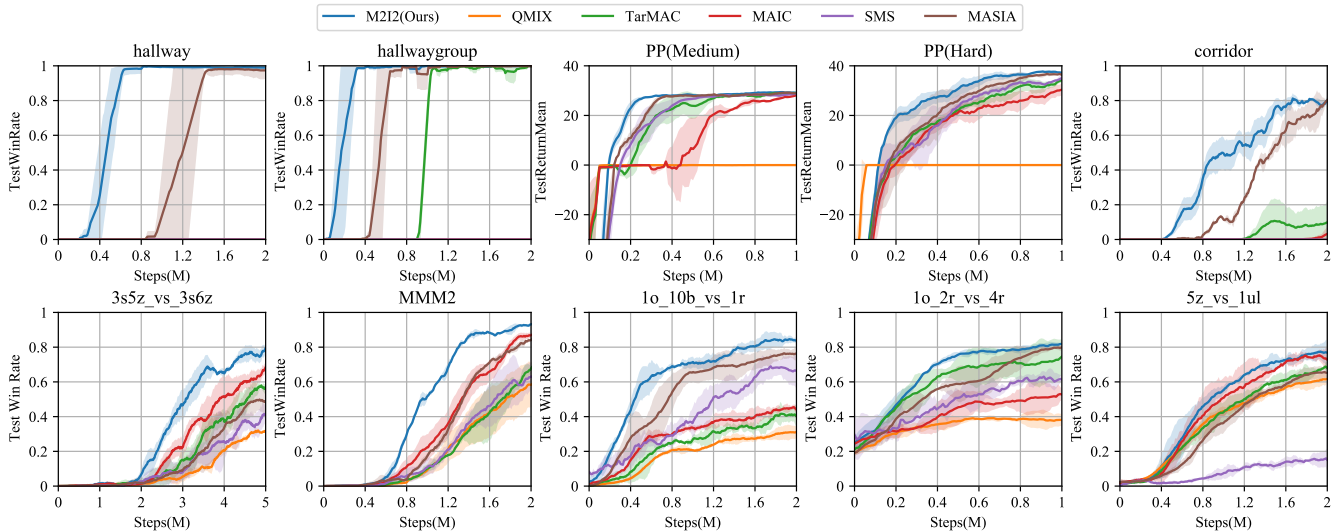


Figure 2: Performance on multiple benchmarks.

multi-agent communication strategies. Detailed descriptions of each environment can be found in **Appendix C**.

Baselines. For comparative analysis, we select a diverse set of baselines. This includes QMIX (Rashid et al. 2018), a well-established MARL algorithm that operates without a communication mechanism. To assess our method’s performance in the context of communication-enhanced MARL, we also include contemporary state-of-the-art communication methods: TarMAC (Das et al. 2019), MAIC (Yuan et al. 2022), SMS (Xue et al. 2022), and MASIA (Guan et al. 2022). Each of these baselines represents a significant stride in the development of communication strategies within the MARL framework, providing a robust backdrop for evaluating the efficacy and innovation of our proposed approach.

Hyperparameters. To ensure reproducibility, the intricate details of our method’s architecture, and our hyperparameter choices are extensively detailed in the **Appendix C**.

5.2 Performance (RQ1)

Our evaluation begins with a comparative analysis of the learning curves of M2I2 against a range of baseline methods across diverse environments. This comparison is aimed at assessing the comprehensive performance of M2I2. As depicted in Figure 2, M2I2 demonstrates a notable performance advantage, consistently outperforming all baselines by a significant margin in each tested environment, indicating M2I2’s strong applicability across scenarios of varying complexity. Specifically, in Hallway, where the reward signals of environment is sparse, many methods exhibit poor performance or fail to learn effectively. In contrast, M2I2 rapidly achieves a 100% win rate. This success can be attributed to our proposed auxiliary tasks, which appear to significantly aid agents in understanding the locations and intentions of their teammates. In PP, where the communication-free method QMIX struggles, most communication methods demonstrate effectiveness. Notably, M2I2

Communication Efficiency	Hallway	PP	SMAC	SMAC-Communication
TarMAC	49.6%	32.32	19.1%	17.4%
MAIC	0.0%	29.75	27.1%	10.1%
SMS	0.0%	51.63	13.7%	41.8%
MASIA	98.6%	32.52	46.5%	28.5%
M2I2(Ours)	165.6%	55.76	98.7%	59.3%

Table 1: Communication Efficiency

achieves the best sample efficiency, swiftly identifying the optimal policy. In SMAC and SMAC-Communication, several full communication methods face challenges in scenarios with large joint observation spaces. For instance, TarMAC shows competence in *1o_2r_vs_4r* and *5z_vs_1ul* but underperforms in *corridor* and *1o_10b_vs_1r*. This could be attributed to the naive approach of these methods in feeding observations from all agents directly into the policy network, thereby increasing the complexity of policy learning. In contrast, M2I2 consistently excels in all six SMAC scenarios, irrespective of the varying difficulties, number of agents, and terrain types. This further underscores the broad applicability and potency of M2I2 in diverse multi-agent communication contexts.

5.3 Efficiency (RQ1)

Efficiency is a long-standing issue in multi-agent communication, as many real-world applications operate under limited communication resources. Therefore, it is crucial to achieve promising performance while maintaining a low communication resource cost. Notably, the performance of M2I2, as reported in Figure 2, was achieved with a 60% communication frequency, where 60% is a hyper parameter defined by our proposed top-k mechanism in **Section 4.1**. To further understand the communication efficiency of M2I2, we adopted a mechanism inspired by MAGIC (Niu, Paleja,

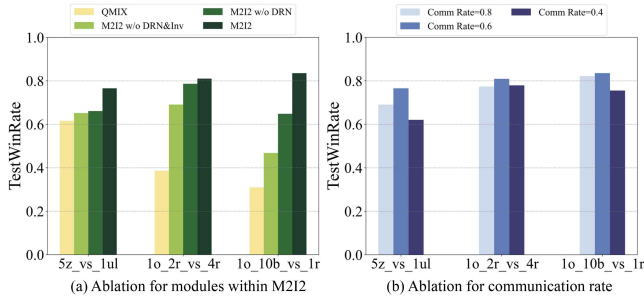


Figure 3: Ablation.

and Gombolay 2021) to measure communication efficiency. Specifically, we calculated the performance improvement for each communication algorithm by subtracting the baseline performance of their communication-free versions. For the SMS algorithm, the communication-free baseline used was DOP (Wang et al. 2020), while for other algorithms, QMIX served as the baseline. Subsequently, we examined the communication frequency for each method. M2I2 and SMS both operated at approximately 60% communication frequency, in contrast to other methods which utilized 100% communication frequency. Finally, we calculated the communication efficiency for each method by dividing the performance improvement by the communication frequency. As indicated in Table 1, M2I2 demonstrated a substantial lead in communication efficiency across all tested scenarios, further validating its effectiveness. This analysis not only underscores M2I2’s ability to maintain high performance with reduced communication demands but also highlights its significant advantages in terms of resource efficiency.

5.4 Ablation (RQ2)

In order to understand the contribution of each module within M2I2, we conduct an ablation study across three SMAC-Communication scenarios. The evaluated configurations are as follows: **M2I2** is our comprehensive method as proposed in the study. **QMIX** acts as a baseline, representing the fundamental functionality devoid of M2I2’s enhancements. **M2I2 w/o DRN** is a variant of M2I2 operates without DRN and top-k filter mechanism. Instead, the observation level masking (i.e. when to communicate) is generated randomly during both the training and sampling processes. **M2I2 w/o DRN & INV** is a further simplified version of M2I2, excluding both the DRN and inverse loss, retaining only the mask state modeling. The results, as depicted in Figure 3(a), highlight the consistent performance improvements attributable to each component across the three scenarios. This underscores the effectiveness of our proposed auxiliary tasks and the DRN in enhancing the overall functionality of M2I2. The clear distinction in performance between these configurations serves to validate the integral role each module plays in the efficacy of the M2I2 framework.

Furthermore, to gain insight into how varying communication frequencies impact M2I2’s performance, we executed an ablation study with communication rates set at 0.8, 0.6, 0.4. The findings, depicted in Figure 3(b), consis-

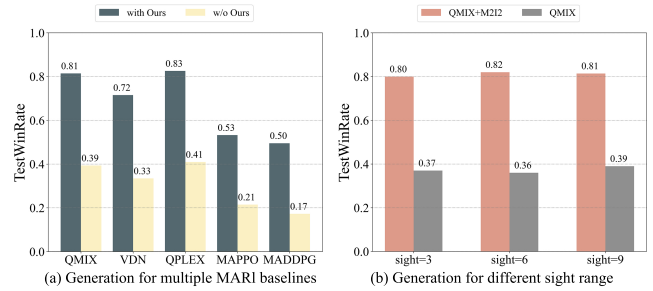


Figure 4: Generation.

tently show the best performance at a communication rate of 0.6. This result suggests that an excessively high communication rate can introduce redundant and misleading information, whereas too low a rate may lead to critical information being overlooked. Intriguingly, reducing information by 0.6 using the meta mask still outperforms a random mask reduction of 0.4, underscoring the meta mask’s proficiency in discerning and prioritizing key information. This delicate balance achieved by M2I2, efficiently filtering out non-essential data while preserving crucial information, significantly enhances the overall communication efficiency in complex multi-agent environments.

At last, to gain deeper insights into the selectively masking process utilized by M2I2, we conducted visualizations to identify which observations are most frequently masked. Additionally, we utilized t-SNE (Van der Maaten and Hinton 2008) to project the learned representation vectors onto a two-dimensional plane. For a comprehensive presentation of these findings, please refer to **Appendix D**.

5.5 Generation (RQ3)

Our previous experiments have conclusively shown M2I2’s robust performance in a variety of environments, encompassing scenarios with diverse complexities and scales. Building on this, we extend our evaluation of M2I2 to assess its generality across various MARL baselines, including QMIX, VDN, QPLEX, MAPPO and MADDPG. To provide a clear representation, we present the test win rates for the scenario *1o_2r_vs_4r* in Figure 4(a). Remarkably, M2I2 demonstrates consistently superior performance across all these baselines, often achieving a significant margin of improvement. This observation shows that M2I2 is effective not only with off-policy algorithms but also with on-policy approaches, and not only with Q-learning methods but also with policy gradient methods, demonstrating M2I2’s broad applicability and effectiveness within the MARL domain. Additionally, we extend M2I2’s application to scenarios featuring varying sight ranges. The results, as depicted in Figure 4(b), confirm that M2I2 not only adapts well but also maintains consistent performance improvements across different sight ranges, further underscoring its versatility and efficacy in enhancing MARL strategies.

6 Conclusion

In this work, we delve into the complexities of multi-agent information integration. We introduce M2I2, an approach that incorporates two auxiliary tasks to enhance communication efficiency. We specifically design a MAE and an inverse model. These elements play a crucial role in guiding the processes of information filtering and integration, thereby significantly enhancing the agents' ability to navigate uncertain environments and dynamically adapt to their teammates. To substantiate our claims, we conduct exhaustive experiments across a multitude of benchmarks. The results from these tests not only validate the effectiveness of M2I2 but also its efficiency and adaptability in various multi-agent scenarios.

References

- Andrychowicz, O. M.; Baker, B.; Chociej, M.; Jozefowicz, R.; McGrew, B.; Pachocki, J.; Petron, A.; Plappert, M.; Powell, G.; Ray, A.; et al. 2020. Learning dexterous in-hand manipulation. *The International Journal of Robotics Research*, 39(1): 3–20.
- Das, A.; Gervet, T.; Romoff, J.; Batra, D.; Parikh, D.; Rabbat, M.; and Pineau, J. 2019. Tarmac: Targeted multi-agent communication. In *International Conference on Machine Learning*, 1538–1546.
- Devlin, J.; Chang, M.; Lee, K.; and Toutanova, K. 2019. BERT: Pre-training of Deep Bidirectional Transformers for Language Understanding. In Burstein, J.; Doran, C.; and Solorio, T., eds., *Proceedings of the 2019 Conference of the North American Chapter of the Association for Computational Linguistics: Human Language Technologies, NAACL-HLT 2019, Minneapolis, MN, USA, June 2-7, 2019, Volume 1 (Long and Short Papers)*, 4171–4186. Association for Computational Linguistics.
- Ding, Z.; Huang, T.; and Lu, Z. 2020. Learning individually inferred communication for multi-agent cooperation. *Advances in Neural Information Processing Systems*, 33: 22069–22079.
- Etel, E.; and Slaughter, V. 2019. Theory of mind and peer cooperation in two play contexts. *Journal of Applied Developmental Psychology*, 60: 87–95.
- Guan, C.; Chen, F.; Yuan, L.; Wang, C.; Yin, H.; Zhang, Z.; and Yu, Y. 2022. Efficient Multi-agent Communication via Self-supervised Information Aggregation. *Advances in Neural Information Processing Systems*, 35: 1020–1033.
- He, K.; Chen, X.; Xie, S.; Li, Y.; Dollár, P.; and Girshick, R. 2022. Masked autoencoders are scalable vision learners. In *Proceedings of the IEEE/CVF conference on computer vision and pattern recognition*, 16000–16009.
- Kim, D.; Moon, S.; Hostallero, D.; Kang, W. J.; Lee, T.; Son, K.; and Yi, Y. 2019. Learning to schedule communication in multi-agent reinforcement learning. *arXiv preprint arXiv:1902.01554*.
- Leurent, E. 2018. A survey of state-action representations for autonomous driving.
- Li, J.; Qiang, W.; Zheng, C.; Su, B.; and Xiong, H. 2022. MetAug: Contrastive Learning via Meta Feature Augmentation. In Chaudhuri, K.; Jegelka, S.; Song, L.; Szepesvári, C.; Niu, G.; and Sabato, S., eds., *International Conference on Machine Learning, ICML 2022, 17-23 July 2022, Baltimore, Maryland, USA*, volume 162 of *Proceedings of Machine Learning Research*, 12964–12978. PMLR.
- Liu, F.; Liu, H.; Grover, A.; and Abbeel, P. 2022. Masked autoencoding for scalable and generalizable decision making. *Advances in Neural Information Processing Systems*, 35: 12608–12618.
- Liu, S.; Davison, A.; and Johns, E. 2019. Self-supervised generalisation with meta auxiliary learning. *Advances in Neural Information Processing Systems*, 32.
- Lowe, R.; Wu, Y. I.; Tamar, A.; Harb, J.; Abbeel, O. P.; and Mordatch, I. 2017. Multi-agent actor-critic for mixed cooperative-competitive environments. In *Advances in neural information processing systems*, 6379–6390.
- Niu, Y.; Paleja, R. R.; and Gombolay, M. C. 2021. Multi-Agent Graph-Attention Communication and Teaming. In *AAMAS*, 964–973.
- Oliehoek, F. A.; Amato, C.; et al. 2016. *A concise introduction to decentralized POMDPs*, volume 1. Springer.
- Osband, I.; Blundell, C.; Pritzel, A.; and Van Roy, B. 2016. Deep exploration via bootstrapped DQN. In *Advances in neural information processing systems*, 4026–4034.
- Rashid, T.; Samvelyan, M.; De Witt, C. S.; Farquhar, G.; Foerster, J.; and Whiteson, S. 2018. QMIX: Monotonic value function factorisation for deep multi-agent reinforcement learning. *arXiv preprint arXiv:1803.11485*.
- Samvelyan, M.; Rashid, T.; de Witt, C. S.; Farquhar, G.; Nardelli, N.; Rudner, T. G.; Hung, C.-M.; Torr, P. H.; Foerster, J.; and Whiteson, S. 2019. The starcraft multi-agent challenge. *arXiv preprint arXiv:1902.04043*.
- Silver, D.; Hubert, T.; Schrittwieser, J.; Antonoglou, I.; Lai, M.; Guez, A.; Lanctot, M.; Sifre, L.; Kumaran, D.; Graepel, T.; et al. 2018. A general reinforcement learning algorithm that masters chess, shogi, and Go through self-play. *Science*, 362(6419): 1140–1144.
- Silver, D.; Schrittwieser, J.; Simonyan, K.; Antonoglou, I.; Huang, A.; Guez, A.; Hubert, T.; Baker, L.; Lai, M.; Bolton, A.; et al. 2017. Mastering the game of go without human knowledge. *nature*, 550(7676): 354–359.
- Singh, A.; Jain, T.; and Sukhbaatar, S. 2018. Learning when to communicate at scale in multiagent cooperative and competitive tasks. *arXiv preprint arXiv:1812.09755*.
- Sukhbaatar, S.; Szlam, A.; and Fergus, R. 2016. Learning Multiagent Communication with Backpropagation. In *Proceedings of the 30th International Conference on Neural Information Processing Systems, NIPS'16*, 2252–2260. Red Hook, NY, USA: Curran Associates Inc. ISBN 9781510838819.
- Sun, C.; Wu, B.; Wang, R.; Hu, X.; Yang, X.; and Cong, C. 2021. Intrinsic Motivated Multi-Agent Communication. In *Proceedings of the 20th International Conference on Autonomous Agents and MultiAgent Systems, AAMAS '21*, 1668–1670. Richland, SC: International Foundation for Autonomous Agents and Multiagent Systems. ISBN 9781450383073.

Van der Maaten, L.; and Hinton, G. 2008. Visualizing data using t-SNE. *Journal of machine learning research*, 9(11).

Vaswani, A.; Shazeer, N.; Parmar, N.; Uszkoreit, J.; Jones, L.; Gomez, A. N.; Kaiser, L.; and Polosukhin, I. 2017. Attention is All You Need.

Vinyals, O.; Babuschkin, I.; Czarnecki, W. M.; Mathieu, M.; Dudzik, A.; Chung, J.; Choi, D. H.; Powell, R.; Ewalds, T.; Georgiev, P.; et al. 2019. Grandmaster level in StarCraft II using multi-agent reinforcement learning. *Nature*, 575(7782): 350–354.

Wang, T.; Wang, J.; Zheng, C.; and Zhang, C. 2020. Learning Nearly Decomposable Value Functions Via Communication Minimization. In *ICLR 2020 : Eighth International Conference on Learning Representations*.

Wang, Y.; Han, B.; Wang, T.; Dong, H.; and Zhang, C. 2020. Dop: Off-policy multi-agent decomposed policy gradients. In *International Conference on Learning Representations*.

Xue, D.; Yuan, L.; Zhang, Z.; and Yu, Y. 2022. Efficient Multi-Agent Communication via Shapley Message Value. In Raedt, L. D., ed., *Proceedings of the Thirty-First International Joint Conference on Artificial Intelligence, IJCAI-22*, 578–584. International Joint Conferences on Artificial Intelligence Organization. Main Track.

Yu, C.; Velu, A.; Vinitsky, E.; Gao, J.; Wang, Y.; Bayen, A.; and Wu, Y. 2022. The surprising effectiveness of ppo in cooperative multi-agent games. *Advances in Neural Information Processing Systems*, 35: 24611–24624.

Yuan, L.; Wang, J.; Zhang, F.; Wang, C.; Zhang, Z.; Yu, Y.; and Zhang, C. 2022. Multi-agent incentive communication via decentralized teammate modeling. In *Proceedings of the AAAI Conference on Artificial Intelligence*, volume 36, 9466–9474.

Zhang, S. Q.; Zhang, Q.; and Lin, J. 2019. Efficient communication in multi-agent reinforcement learning via variance based control. In *Advances in Neural Information Processing Systems*, 3235–3244.

Zhang, S. Q.; Zhang, Q.; and Lin, J. 2020. Succinct and robust multi-agent communication with temporal message control. *Advances in Neural Information Processing Systems*, 33: 17271–17282.

A Notations

For clarity and precise symbol definitions, we provide a comprehensive list of notations used in this work in Table. 2.

Notations	
N	a collective of agents
n	number of agents
S	a set of global states
O	accessible local observations
A	available actions
\mathbb{O}	observation function
P	transition function
R	reward function
γ	discount factor
M	the set of messages
s_t	global state at time-step t
o_i^t	observation of agent i at time-step t
m_i^t	message sent by agent i at time-step t
z_i^t	integrated information by agent i at time-step t
a_i^t	selected action of agent i at time-step t
a_t	joint action of all agents at time-step t
s_t'	reconstructed state at time-step t
a_t'	predicted joint-action at time-step t
$\pi(o_i^t, c_i^t)$	local policy
ω_i^t	the importance of agent i 's observed information at time-step t
Q_{tot}	total q-value
\mathcal{L}_{RL}	loss of RL
\mathcal{L}_{RC}	reconstructed loss
\mathcal{L}_{INV}	inverse loss
\mathcal{L}_{M2I2}	M2I2 loss
θ_E	parameters of message encoder
θ_π	parameters of policy network
θ_D	parameters of state decoder
θ_I	parameters of inverse model
θ_{DRN}	parameters of DRN
θ_{trial}	trial parameters for meta learning

Table 2: Notations

B Implementation Details

To explain the communication process and training paradigm, we provide the pseudo-code for M2I2 in Algorithm 1.

C Experimental Setup

All the Result are reported by averaging the results of 5 random seeds. The four test environments of the experiment are shown in Figure 5.

C.1 Environment

Hallway. This task revolves around multiple Markov chains where n are initially distributed randomly across n chains with varying lengths. The goal is for all agents to simultaneously reach the goal state, despite the constraint of partial observability. For increased challenge, n is set to 4, and each chain has a unique length specified as (4, 6, 8, 10). At each time step, an agent has a limited observation of its current position, and it can choose from three actions: move left, move right, or remain stationary. An episode concludes when any agent reaches state g . The agents collectively succeed and receive a shared reward of 1 only if they all reach state g concurrently. Otherwise, the reward is 0.

Hallwaygroup. This is a variant of Hallway which agents are divided into different groups and different groups have to arrive at different times. To intensify the challenge, we escalated the complexity by increasing both the number of agents and the lengths of the Markov chains. Specifically, in the Hallway benchmark, we set the number of agents to 4, with Markov chain

Algorithm 1: M2I2

Initialize replay buffer D ,
Initialize the random parameters of Dimensional Rational Network θ_{DRN} , Message Encoder θ_E , State Decoder θ_D , Inverse Model θ_I and Policy Network θ_π
Set learning rate α and max training episode E
for episode in $1, \dots, E$ **do**
 for each agent i **do**
 Sending Phase:
 Encode importance weight ω_i from observation o_i^t
 Compute the masked importance weight ω'_i with Top-k Scheduler by Equation 2
 Generate the shared message m_i^t with ω'_i and o_i^t by Equation 3
 Receiving Phase:
 Encode the integrated representation z_i^t from the received message by Equation 4
 Make cooperative decisions by Policy Network for a_i^t by Equation 5
 end for
Store the trajectory in replay buffer D
Sample a minibatch of trajectories from D
Compute the reconstructed loss \mathcal{L}_{RC} by Equation 6
Compute the inverse loss \mathcal{L}_{INV} by Equation 7
Compute the reinforcement Loss \mathcal{L}_{RL}
Update the combined set of parameters $\theta = (\theta_E, \theta_D, \theta_I, \theta_\pi)$ by Equation 8
Compute the trail weight θ_{trail} after one gradient update of θ using the M2I2 loss by Equation 10
Update the parameters of Dimensional Rational Network θ_{DRN} by Equation 9
end for

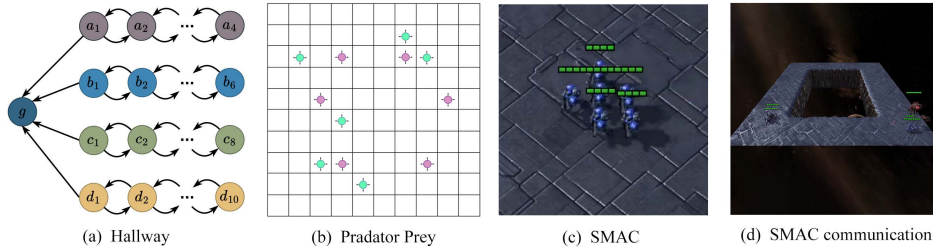


Figure 5: Multiple environments considered in our experiments.

lengths varying as (4,6,8,10). In the Hallwaygroup variant, we increased the number of agents to 7, dividing them into two groups. The lengths of the Markov chains for these two groups were set to (3,5,7) and (4,6,8,10), respectively.

Predator Prey (PP). In this task, the objective for predators is to capture randomly moving preys. Each predator has the ability to navigate in four distinct directions, but their perspectives are limited to local views. The game dynamics involve multiple predators attempting to capture the same prey simultaneously, resulting in a team reward of 1. However, if only a single predator successfully captures a prey, they incur a penalty with a score of -2. The game concludes when all preys have been captured. To introduce varying difficulty levels, different grid sizes and numbers of agents are employed for the Predator-Prey (PP) scenarios. The specific configurations for two PP scenarios are detailed in Table. 3.

Table 3: The configurations of PP scenarios

	<i>Grid size</i>	$n_{predators}$	n_{preys}
Medium	10 * 10	6	6
Hard	15 * 15	8	8

StarCraft Multi-Agent Challenge (SMAC). This task revolves around a series of complex scenarios inspired by StarCraftII, a real-time strategy game. Decentralized agents engage in combat against the built-in AI, each having a limited field of vision restricted to adjacent units. Observations include relative positions, distances, unit types, and health statuses. Agents struggle to perceive the status of entities beyond their immediate vicinity, creating uncertainty. The action space varies across scenarios, often including move, attack, stop, and no-option. During training, global states with coordinates and features of all agents are

accessible. Rewards are based on factors like damage infliction, eliminating units, or victory.

SMAC-Communication. To emphasize the role of communication, we select three super hard maps and further adopt the configuration used in (Wang et al. 2020). The specifics of the chosen scenarios are delineated as follows.

5z_vs_1ul. A team of 5 Zealots faces a formidable Ultralisk. Victory requires mastering a complex micro-management technique involving positioning and attack timing.

1o_10b_vs_1r. In a cliff-dominated terrain, an Overseer spots a Roach. 10 Banelings aim to eliminate the Roach for victory. Banelings can choose silence, relying on the Overseer to communicate its location, testing communication strategy efficiency.

1o_2r_vs_4r. An Overseer encounters 4 Reapers. Allied units, 2 Roaches, must locate and eliminate the Reapers. Only the Overseer knows the Reapers’ location, requiring effective communication for success.

C.2 Network architecture

Module	Architecture
Message Encoder	Q:Linear(obs_dim, 16) K:Linear(obs_dim, 16) V:Linear(obs_dim, 32) RNN(32, 32) Linear(32,8*n_agent)
State Decoder	Linear(8*n_agent,32) Linear(32,state_dim)
Inverse Model	Linear(8*n_agent,64) Linear(128,64) Linear(64,n_agent*n_action)
Policy Network	Linear(obs_dim,32) Linear(32+8*n_agent,32) RNN(32, 32) Linear(32, n_action)
DRN	Linear(obs_dim,32) RNN(32,32) Linear(32,obs_dim)

Table 4: Network architecture of M2I2

C.3 Hyper-parameters

Hyper-Parameters	
epsilon start	1.0
epsilon finish	0.05
epsilon anneal time	50000
buffer size	5000
target update interval	200
hidden dimension for mixing network	32
β	1
mask ratio	0.4

Table 5: Hyper-Parameters of M2I2

D Visualization

To showcase the effectiveness of each module within M2I2, we conduct visualizations to illustrate what features does DRN focus on more, which pieces of observations are masked and what the integrated representation has learned.

D.1 Visualization of weight learnen by DRN

To evaluate the adaptive capability of DRN, we visualized the learned importance of each observation component in Fig. 6 and found that DRN can effectively allocate varying levels of importance across different agent types and observation types.

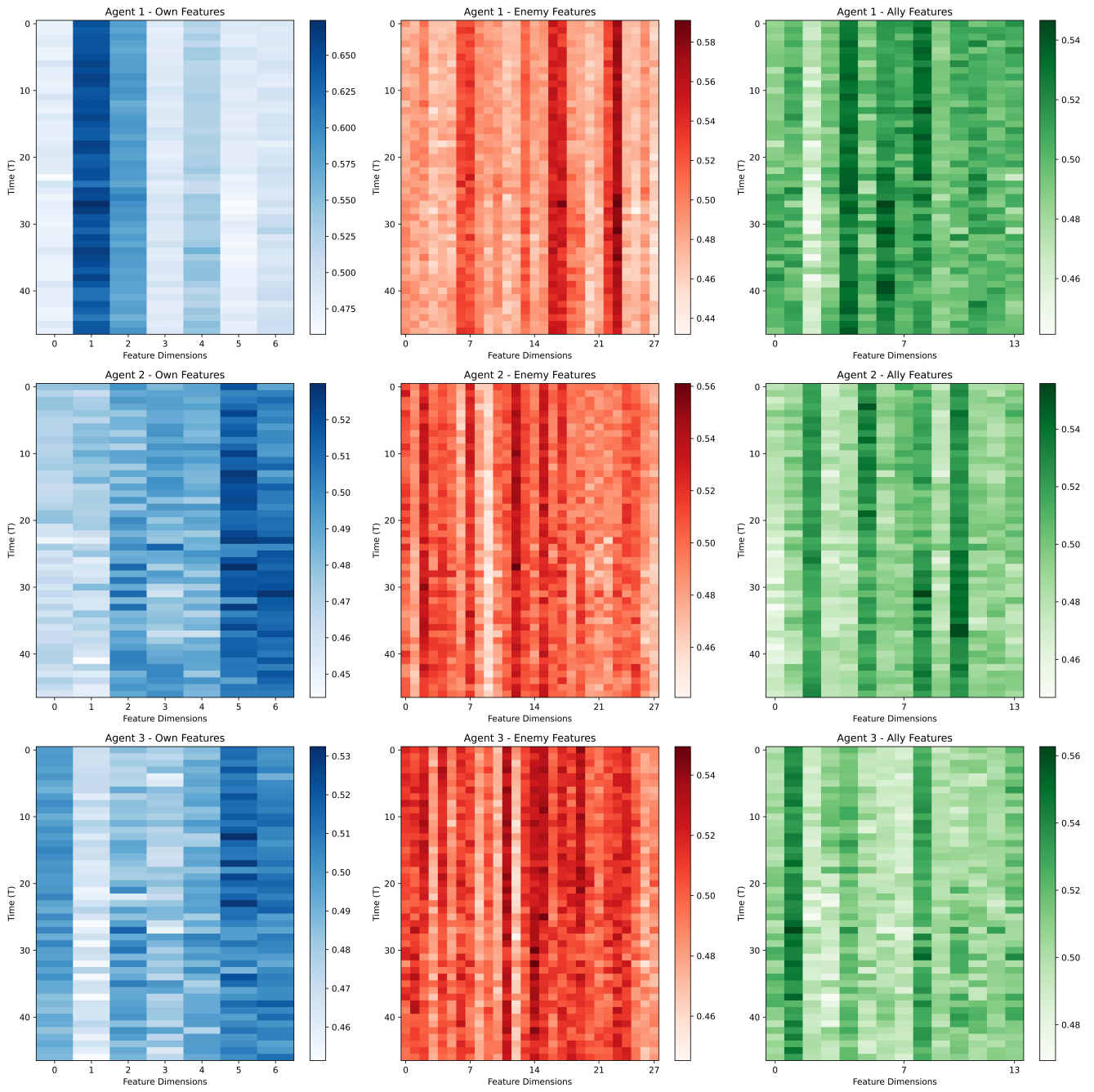


Figure 6: Visualization of weight learn by DRN

Moreover, these importance weights adapt dynamically as time and situations evolve. The detailed analysis can be divided into three-fold:

- **Agent level analysis.** In the task we evaluated, Agent 1 primarily focuses on observing enemy information, while Agents 2 and 3 are tasked with moving towards the enemy’s location to destroy them. The visualization reveals that the ω_i^t matrices for Agents 2 and 3 are more similar to each other and less similar to the matrix for Agent 1. This indicates that DRN differentiates between the significance of various agent types.
- **Observation level analysis.** We found that DRN assigns different levels of importance to various observation dimensions, highlighting its ability to prioritize critical information effectively.
- **Time level analysis.** Lastly, we observed that the importance of certain observations dynamically changes over time, further demonstrating DRN’s adaptive capability in response to evolving situations.

D.2 Visualization of mask probability

To gain deeper insights into the meta-learned mask generating policies (i.e., communication policies), we present a visualization of the mask ratio for different observations in Figure 7. Specifically, we divided each episode into two stages: the first 80% of time steps are categorized as the Explore stage, and the remaining 20% as the Battle stage. During the Explore stage, the agent primarily focuses on moving and sharing information about enemy locations, with an emphasis on exploration and navigation. In the Battle stage, the agent identifies the enemy and engages in combat.

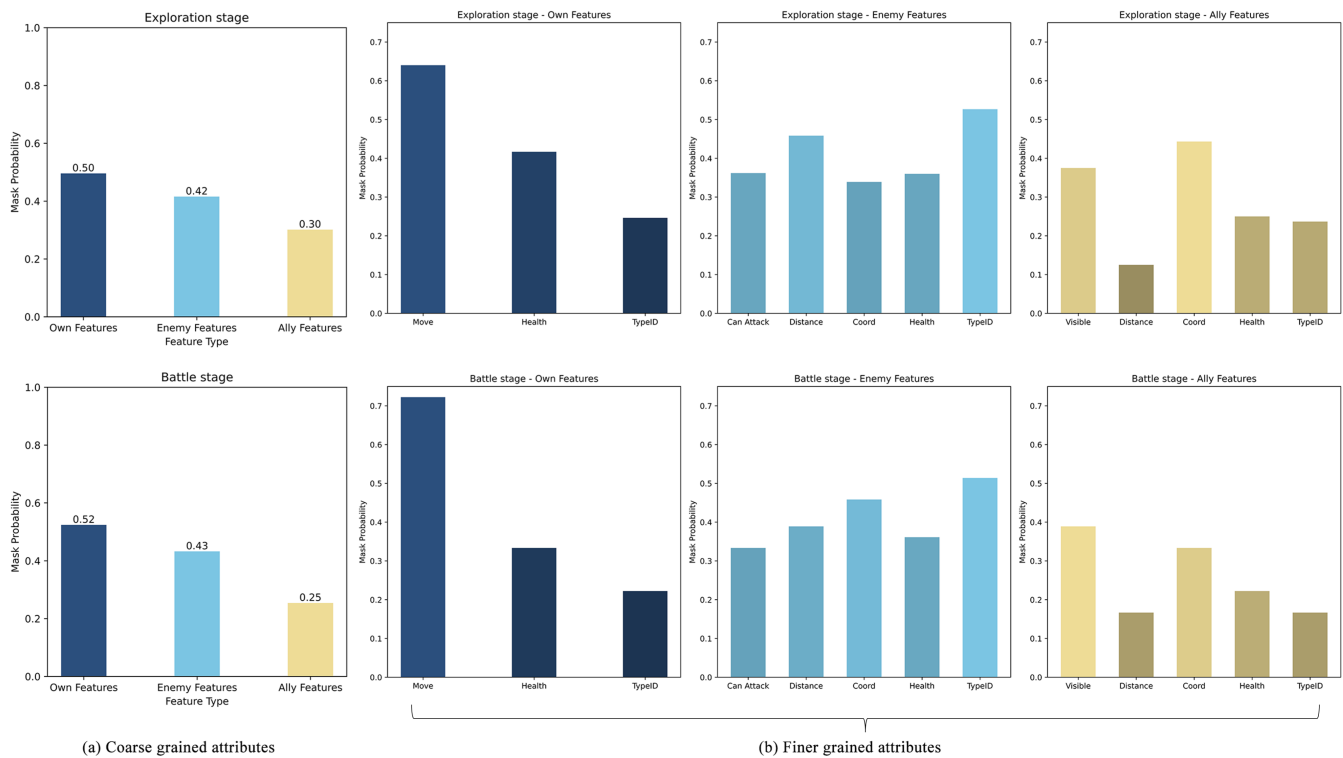


Figure 7: (a) Presents the probability of masking for the three types of observations at different stages. (b) Illustrates the probability of masking for each specific attribute within each observation type across various stages.

At a high level, we categorize the observations into three types: observations of the agent itself, observations of enemy agents, and observations of ally agents. As shown in Figure 7(a), we observe that DRN considers ally features to be more critical for decision-making in both stages, leading to a lower proportion of these features being masked compared to other types of observations.

To gain deeper insights, we further categorized the own, enemy, and ally features into more specific attributes. As depicted in Figure 7(b), we observed that DRN’s masking tendencies shift between the stages depending on the attribute. During the Exploration stage, the agent relies heavily on enemy information for positioning and movement, resulting in the lowest masking rate for enemy location attributes. However, in the Battle stage, as movement becomes less critical, the importance of enemy health information increases, leading to a higher retention of health-related attributes.

Overall, this visualization highlights that DRN dynamically adjusts the importance weights of different observation attributes over time to align with the evolving demands of the task.

D.3 Visualization of learned representations

At last, to visualize what kind of representations the encoder has learned, we use t-SNE (Van der Maaten and Hinton 2008) to project the learned representation vectors into a two-dimensional plane. As illustrated in Figure 6, we conduct a visualization analysis on the map *1o_2r_vs_4r*. To distinguish aggregated representations at different time-steps, we mark larger time-steps with darker shades of the dots. We observe that the aggregated representations can be well distinguished by phases. Projected representations in the seeking phase are far from those in the battle phase, demonstrating that M2I2’s representations exhibit robust discriminability, indicating the model’s nuanced understanding of the environment.

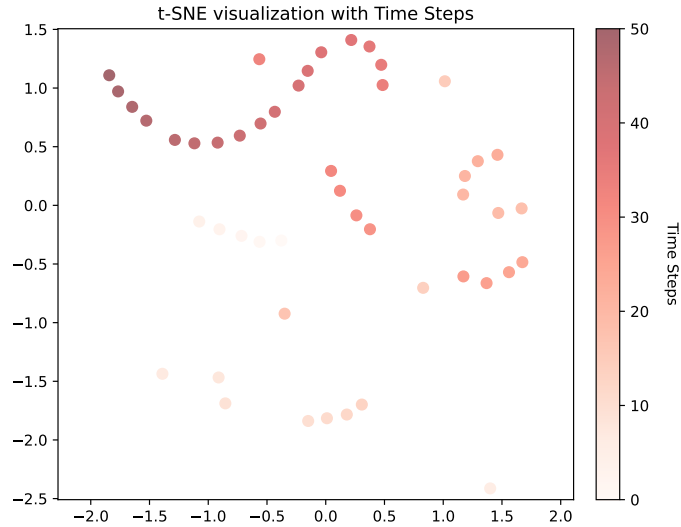


Figure 8: Visualization of learned representations

D.4 Learning curves for self-supervised learning loss

In addition to the visual representation, we provide learning curves for \mathcal{L}_{RC} and \mathcal{L}_{INV} in Figure 9 and Figure 10, respectively. The observed quick convergence of \mathcal{L}_{RC} and \mathcal{L}_{INV} suggests that our masked modeling and inverse model indeed equip agents with the ability to reconstruct global states and infer joint actions based on limited communication resources. These curves offer insights into the training dynamics and convergence of the reconstruction and inverse modeling tasks.

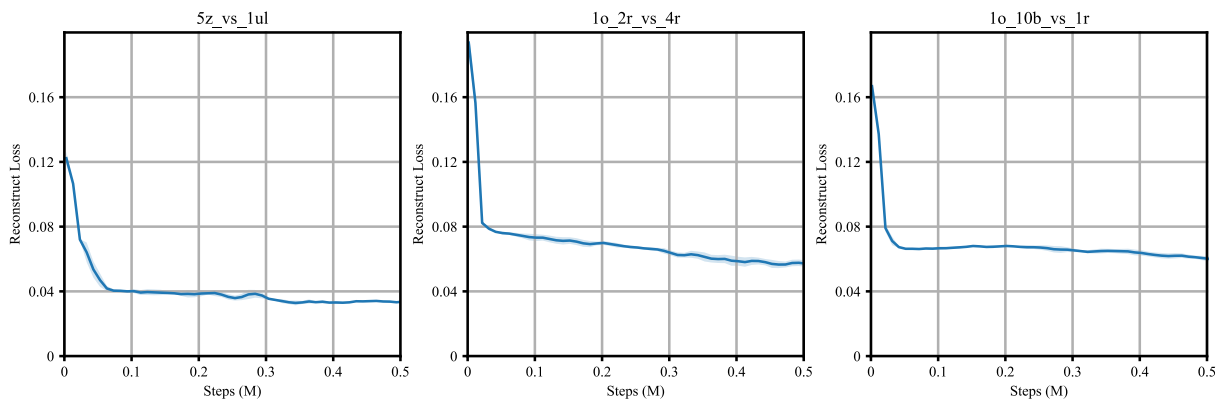


Figure 9: Reconstruct Loss

E Details of Computational Resources

The computational experiments described in this paper were executed on a dedicated high-performance computing cluster to ensure the reproducibility and efficiency of the results. Below, we provide the detail of the computational resources used:

- **GPU Specifications:**

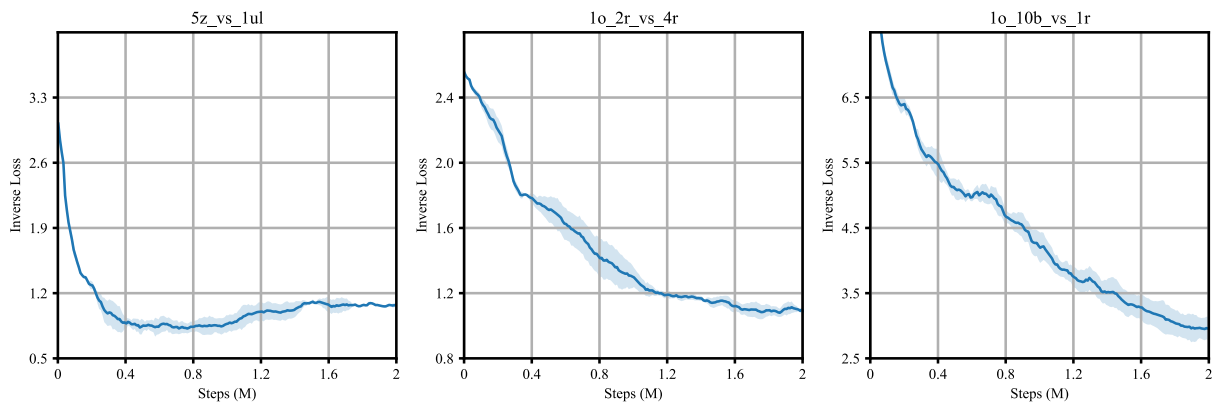


Figure 10: Inverse Loss

- Quantity: 3 NVIDIA TITAN Xps
- Memory: 12 GB GDDR6X per GPU
- **CPU Specifications:**
 - Model: Intel(R) Xeon(R) Silver 4114 CPU
 - Architecture: x86_64
 - Base Clock Speed: 2.20GHz
- **Software and Frameworks:**
 - Operating System: 16.04.1-Ubuntu SMP
 - Machine Learning Libraries: torch 2.1.0

In Table.6 we present the number of models' parameters and running time of our baselines on the *1o_2r_vs_4r*. In the Experiment, M2I2's parameters and training time, 0.82-1.19 and 0.65-1.47 times those of baselines respectively, which indicates its computational efficiency.

	M2I2	MAISA	QMIX	TarMAC	MAIC	SMS
Parameters	182,458	178,348	79,605	123,899	123,017	84,326
Memory/Process	368MIB	358MIB	309MIB	330MIB	325MIB	808MIB
Time/episode	0.45s	0.4s	0.082s	0.15s	0.44s	0.9s

Table 6: Parameters and running time of our baseline